Flickering of the Recurrent Nova T CrB

K. Yankova¹, D. Boneva¹, B. Spassov², M. Minev², R. K. Zamanov²

(Submitted on 15.05.2025; Accepted on 28.08.2025)

Abstract. We report observations of the flickering of the recurrent nova T CrB in UBV bands obtained during three nights in 2024. We find that (1) the optical luminosity of the hot component is in the range of $19-28~\rm L_{\odot}$, which corresponds to a mass accretion rate of $0.6-1.0\times10^{-8}~\rm M_{\odot}~\rm yr^{-1}$, and (2) on a time scale of 1 hour the mass accretion rate varies as \dot{M}_a (max/min) ~ 1.4 . (3) We apply our model to track local deviations from the average accretion rate across the T CrB accretion disk in relation to the observed flickering. The results show that in the optical part of the disk, the obtained values correlate with the observations. The accretion rate variations increase strongly in the internal disk part, which can be interpreted as an indication of interaction processes within the contact zone. The data are available upon request from the authors.

Key words: stars: binaries: symbiotic — novae, cataclysmic variables — accretion, accretion disks — stars: individual: TCrB

1 Introduction

T Coronae Borealis (T CrB) is a member of the symbiotic binary stars class (Allen 1984, Kenyon 1986). Symbiotic binary stars are systems that usually consist of a red giant and a white dwarf companion (Kenyon 1990). There are two known active transfer mechanisms between the components in this binary class. The matter could be transferred by the Roche lobe overflow through the Lagrange point L1 (Frank et al. 2002) or by a stellar wind from the giant component (Boffin 2015, Munari 2019). At a later evolutionary stage, this matter accretes onto the white dwarf primary (Warner 2003). Many symbiotic binaries manifest outburst activity. If these outbursts repeat over time in a binary, the system is classified as a recurrent nova (Webbink et al. 1987, Warner 2003).

T´ CrB is classified as one of the few known recurrent novae in the Galaxy (Warner 1995, Schaefer 2010), based on the registered outbursts in the historical light curves of the observations (Schaefer 2023). Up to now, two outburst events of this binary have been registered in a period of 80 years. The first one was in 1866 (Huggins 1866), while the second outburst appeared 80 years later in 1946 (Payne - Gaposchkin 1964).

Observations of T CrB have shown the existence of flickering with various photometric amplitudes in different bands (Gromadzki et al. 2006). Flickering is known as aperiodic and irregular variations in the light curve on timescales of a seconds to few minutes with amplitude of a few 0.1 magnitudes (Bruch 1992). Flickering with the largest amplitudes of 0.1-0.5 mag are observed in the U band (Sokoloski et al. 2001, Zamanov et al. 2004), while in the B and V bands the amplitudes are smaller (Hric et al. 1998). The amplitudes of the brightness variations could increase to ~ 2 mag in the U band, against the

¹Space Research and Technology Institute, Bulgarian Academy of Sciences, BG-1113, Sofia, Bulgaria

²Institute of Astronomy and National Astronomical Observatory, Bulgarian Academy of Sciences, Tsarigradsko Shose 72, BG-1784 Sofia, Bulgaria

shorter wavelengths (Hric et al. 1998). Strong flickering activity, similar to that observed in Cataclysmic variables, is also detected at short wavelengths (Zamanov & Bruch 1998). The UV and X-rays spectral emissions of T CrB confirm the presence of flickering activity (Zhekov & Tomov, 2019). The physical mechanisms of the flickering's origin are still under consideration. The most promising models during the years proposed accretion onto the white dwarf as a main source of the flickering. The sources could also be: an unsteady accretion through a bright spot or boundary layer (Warner & Nather 1971, Bruch 1992); unstable mass transfer (Bruch & Duschl 1993) or turbulence in the accretion disk as a mechanism for an angular momentum transport (Balbus & Hawley 1998, Dobrotka et al. 2010). The origin of flickering in T CrB is also proposed to be coming from the vicinity of the WD (Zamanov & Bruch 1998).

By analysing the ellipsoidal variability the obtained value for the mass of the white dwarf is $1.2 \pm 0.2 M_{\odot}$ (Belczynski & Mikolajewska 1998) and for the red giant mass it is $0.8 \pm 0.2 M_{\odot}$ (Belczynski & Mikolajewska 1998). Using the radial velocity measurements, the solution for the mass values gives $1.37 \pm 0.13 M_{\odot}$ for the white dwarf and $1.12 \pm 0.13 M_{\odot}$ for the red giant, and for the system inclination $i \simeq 67^{\circ}$ (Stanishev 2004). The luminosity of the white dwarf is in the range of $5-40L_{\odot}$ (Cassatella et al. 1985, Selvelli et al. 1992). The red giant's spectral type is M4III (Mürset and Schmid 1999).

The binary orbital period was calculated using radial velocity measurements. The average value that can be adopted is 227.5687 ± 0.0099 days (Kenyon & Garcia 1986; Leibowitz, et al. 1997; Fekel et al. 2000). The distance to the object is determined to be 890 pc (Gaia DR3 data and Bailer-Jones et al. (2021)) and 914 pc (Schaefer 2022). At the distance of 890 pc, the rate of accretion is estimated for different time intervals. For the years between 1978 and 1990, the average accretion rate is found to be $9.6 \times 10^{-9} M_{\odot} yr^{-1}$ (Selvelli et al. 1992, Stanishev et al. 2004). During the high state of the object (from 1980 to 1988) the accretion rate was $1.1 \times 10^{-8} M_{\odot} yr^{-1}$, while in low states (from 1978 to 1980 and 1988 to 1990) it was $1.5 \times 10^{-9} M_{\odot} yr^{-1}$ (Stanishev et al. 2004). The measured value of the accretion rate between the two nova outbursts by Luna et al. (2019) is $\approx 0.7 \times 10^{-9} M_{\odot} yr^{-1}$.

Accretion disk processes, like variations in the mass-transfer stream rate or in the accretion rate, and disk instabilities (most often the thermal-viscous instability and the tidal instability, Lasota (2001), Smak (2000)) are usually related to upcoming outburst activity in these objects.

In accordance with the past recurrent outburst activity of T CrB with a period of ≈ 80 years, we could expect the next event to happen in the years between mid 2025 and late 2026 (Luna et al. 2020, Schaefer 2023).

Following the above presented time intervals of sequential activities of outbursts, high and low states, we focus on the flickering that appeared in the system. In this work, we present simultaneous observations of the intra-night variability of T CrB in the Johnson U, B and V bands, estimate mass accretion rate onto the white dwarf, and model the accretion disk behavior. We track the accretion rate fluctuations across the disk, which cause flickering variations in luminosity.

2 Observations

The new observations of T CrB were performed with the 50/70 cm Schmidt telescope (Tsvetkov et al. 1987) and the 1.5 m photometric telescope (Minev et al. 2024) of the Rozhen National Astronomical Observatory, by alternating U, B and V filters, during three nights in 2024. The telescopes were equipped with CCD cameras and rotating filter wheels. Data reduction was performed by means of IRAF following the standard recipes for processing of CCD images and aperture photometry. We used comparison stars form the list of Henden & Munari (2006). The journal of observations and results from the photometry are summarized in Table 1. It lists the date and duration of the observational runs, the respective number of exposures in each band and the exposure times, the minimum, maximum, and average magnitudes of the target, the standard deviation of the run, and the typical observational errors. Our new observations are presented in Fig. 1.

date telescope	UT start-end	band	N_{pts} exposure	min [mag]	max [mag]	0	stdev	merr
2024-07-07 50/70cm	19:34 - 01:09	U B V	$\begin{array}{c} 247 \text{x} 30 \text{s} \\ 246 \text{x} 10 \text{s} \\ 246 \text{x} 5 \text{s} \end{array}$	11.069	11.537		0.070	0.010
2024-08-23 1.5m	18:20 - 19:50	${\rm U} \\ {\rm B} \\ {\rm V}$	0		11.293	11.5912 11.2478 9.9243	0.018	0.005
2024-09-03 1.5m	18:34 - 19:28	U B V	000		11.210	11.1989 11.1281 9.8887	0.041	0.005

Table 1: Journal of observations.

3 Mass accretion rate onto the white dwarf

From the UBV data we calculate the dereddened magnitude U_0 , and the dereddened colours of the hot component. We apply the following procedure in order to estimate the luminosity of the hot component:

1. We correct the observed magnitudes for the interstellar extinction, adopting E(B-V)=0.07 (Nikolov 2022). To convert the observed magnitudes in fluxes, we use the calibration for a zero magnitude star: $F_0(B)=6.13268\times 10^{-9}$ erg $cm^{-2}s^{-1}$ Å⁻¹, $\lambda_{eff}(B)=4371.07$ Å, $F_0(V)=3.62708\times 10^{-9}$ erg $cm^{-2}s^{-1}$ Å⁻¹ and $\lambda_{eff}(V)=5477.70$ Å as given in the Spanish virtual observatory Filter Profile Service (Rodrigo & Solano 2020).

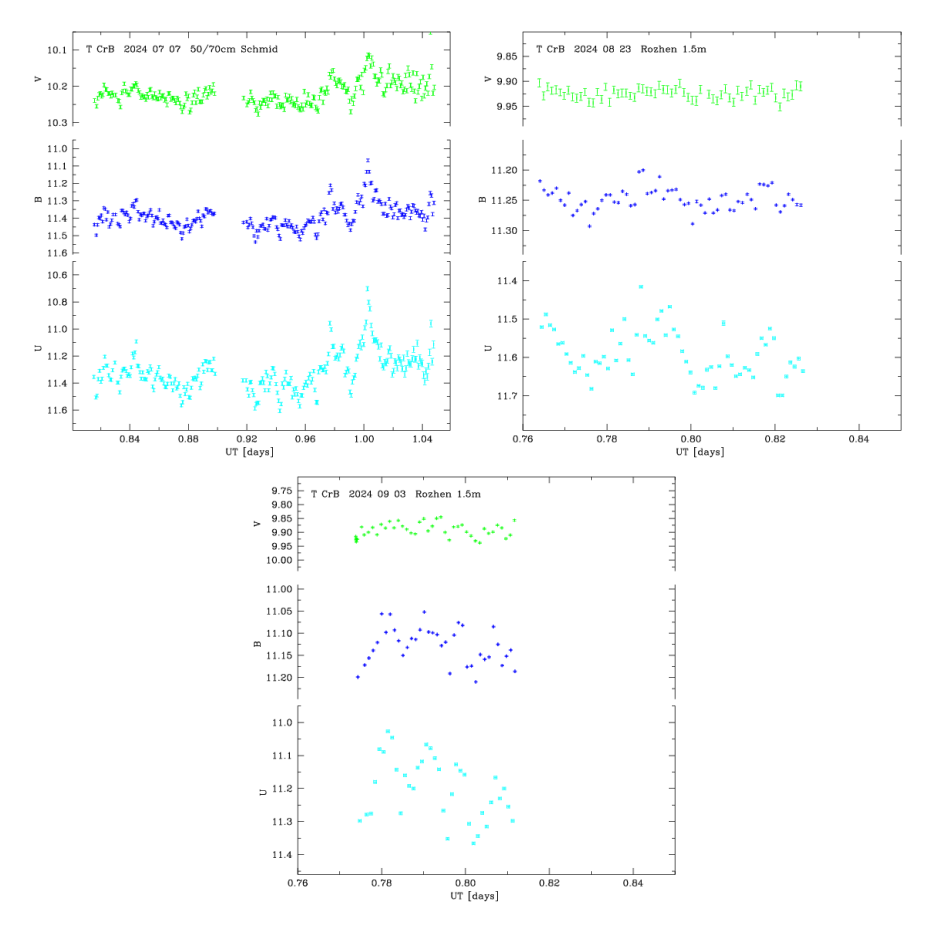


Fig. 1: UBV observations of the flickering of TCrB (green - V band, blue - B band, cyan - U band). Typical amplitude of variability on a time scale of 1 hour is 0.4 mag in U band, 0.25 in B band, 0.1 in V band. More details can be found in Table 1.

- 2. We convert the dereddened magnitudes into fluxes using the calibrations for generic Bessell UBV filters given in Rodrigo & Solano (2020).
 - 3. We subtract the contribution of the red giant.
 - 4. We calculate U_0 , $(U-B)_0$ and $(B-V)_0$ of the hot component.
- 5. Using $(U-B)_0$ and $(B-V)_0$ and the calibration for a black body (Table 18 in Strayzys 1992), we calculate the effective temperature.
- 6. Using a distance d = 914 pc (Schaefer 2022) and the dereddened magnitude U_0 , we calculate the effective radius and the optical luminosity of the

Table 2: Temperature T[K], effective radius R_{eff} , luminosity L/L_{\odot} , and mass accretion rate \dot{M}_a of T CrB.

date		T[K]	R_{eff}	L/L_{\odot}	\dot{M}_a [10 ⁻⁸ \dot{M}_\odot yr ⁻¹]	\dot{M}_a
					$[10^{-8} \ \mathrm{M}_{\odot} \ \mathrm{yr}^{-1}]$	max/min
20240707	min	7106	2.916	19.4	0.69	
	max	8959	2.228	28.7	1.01	1.47
	aver	8049	2.381	21.3	0.75	
20240823	min	6695	3.180	18.2	0.64	
	max	7013	3.018	19.8	0.70	1.08
	aver	6813	3.133	19.0	0.67	
20240903	min	7802	2.489	20.6	0.73	
	max	8522	2.324	25.5	0.90	1.24
	aver	7399	3.126	26.3	0.93	

hot component.

7. From the luminosity of the hot component we estimate the mass accretion rate. More details can be found in Zamanov et al. (2023).

Table 2 gives the date of the observational run, the temperature of the hot component, its effective radius, and estimated mass accretion rate. These are calculated for the minimum, maximum, and average brightness for each night. The typical error of the temperature is less than ± 500 K. The error of the estimated luminosity is about $\pm 7\%$. For the average mass accretion we obtain $\approx 10^{-8} \text{ M}_{\odot} \text{ yr}^{-1}$. As a result of the flickering \dot{M}_a varies as $\dot{M}_a(\text{max/min})=1.47$ for 2024-07-07, $\dot{M}_a(\text{max/min})=1.08$ for 2024-08-23, and $\dot{M}_a(\text{max/min})=1.24$ for 2024-09-03.

4 Mass accretion rate into model solution of T CrB disk

In this section, we present our modelling of the rates of accretion in different active disk zones, with relation to the flickering variations in U and B bands. The occurrence of the flickering is expected at the bright spot or boundary layer. They practically coincide with two of the disk's active areas. The disk usually forms five active zones (AZ) (Yankova 2025), which are developed into two types - internal and adjacent. In each of the zones, the activity is the result of the sudden change in the physical parameters in the stream, caused by the interactions between the components of the system (jets-accretor-disk-corona), or amendments of the disk structure. Here we consider the following internal zones:

• The real active zone is formed internally in the disk, when advection develops there. Advection is the result of the interaction of the plasma with the field and causes intra-structural changes in the disk flow. Therefore, the accretion rate increases by up to about 15 percent locally (at the same radius)

compared to a disk without the advection action. The active zone is divided into two parts (Yankova 2019): the plateau in the luminosity indicates the outer active zone, in which the advection conceals the activity; luminosity increase in the inner active zone ($x < 0.4, x = r/R_{out}R_{\odot}, R_{out} \sim 100R_{\odot}$), where the activity becomes observable (see Fig.2). The reason for this is a smooth transition between two advective modes in the disk. The non-dominant advection in the outer regions retains the released energy in the flux, using it to self-induce and thus suppress the disk activity. In the inner regions it is replaced by an advective regime, which can no longer control the energy distribution in the disk flow so effectively, and then the activity can be observable.

- External contact AZ: The outer contact active zone is formed by the interaction of the transfer inflow with the outer regions of the disk and is commonly known as a spot or a hot line.
- Internal contact AZ: develops when the disk reaches the accretor, its envelope or magnetosphere. It is formed upon the interactions in there, depending on the physical parameters of the disk, for each object. In the case of T CrB the accretor forms a shell (Yankova et al. 2025) and the activity is caused by the interactions of the inner disk layers with the outer parts' envelope.

We can use the model, presented in (Yankova 2009, Yankova et al. 2014), as a way to track changes in the accretion rate across the disk for the largest deviation in values. Accretion rate fluctuations will cause a local increase in the released energy of the disk. The re-radiating of the additional energy quantities rises at this radius. This will be reflected in a short-term increase in the luminosity, which can be registered as flickering in the observations. In terms of the model, we have:

$$L_{id}(x) \approx L_0 f_1(x) f_4(x) x^{-0.5} \left[\left(\frac{f_2(x)}{f_{\varphi}(x)} \right)^2 + 1 \right]^{3/2}$$
 (1)

and

$$\dot{M}(x) = \dot{M}_0 x f_4(x) f_1(x) f_2(x) \tag{2}$$

Here $F_i(x)$ are respectively the dimensionless functions of the parameters: $f_1(x)$ the equatorial density distribution; $f_2(x)$ and $f_{\varphi}(x)$ are the two velocity distributions - radial and angular, $f_4(x)$ - the disk semi-thickness H, $L_{id}(x)$ - the disk luminosity distribution, and L_0 - the initial luminosity; \dot{M}_0 is the initial accretion rate on the outer edge.

The view of the radial distribution of the luminosity, obtained by the model, is presented in Figure 2.

Then from Eqs. 1 and 2 we obtain the next two expressions for the flickering:

$$\left(\frac{L_{fl}}{L_{id}}\right)^{2/3} = \frac{xf_{fl}^2 + 1}{xf_2^2 + 1} \tag{3}$$

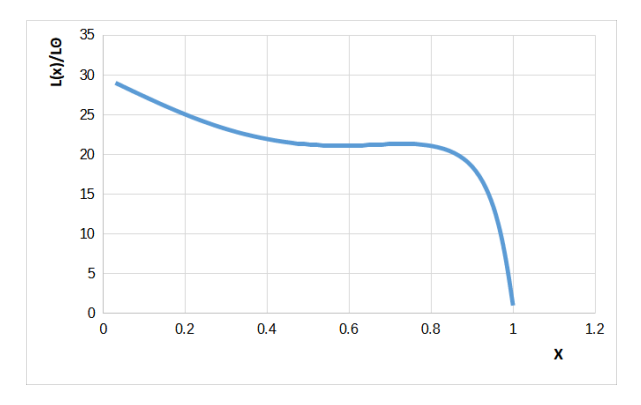


Fig. 2: The radial luminosity distribution by the model solution of T CrB accretion disk.

$$\frac{\dot{M}_{max}}{\dot{M}_{min}} = \frac{f_{fl}}{f_2} \tag{4}$$

Further, by Eqs. 3 and 4, we have:

$$\frac{\left(\frac{\dot{M}_{max}}{\dot{M}_{min}}\right)^2 + x^{-1}f_2^{-2}}{1 + x^{-1}f_2^{-2}} = \left(\frac{T_{max}}{T_{min}}\right)^{8/3} \tag{5}$$

where $\dot{M}_{max}/\dot{M}_{min}$ are the accretion rate fluctuations, which cause flickering changes in the luminosity L_{fl} ; f_{fl} are fluctuations in the average flow velocity distribution; T_{max} and T_{min} - the temperatures in the maxima and minima, respectively.

We use Table 2 and extrapolate from the tabulated values in (Zamanov et al. 2023) to obtain estimates in both observational spectra. We can see the distributions of the accretion rate in the different regions of the disk, for U band (Eqs. 6-8) and for B band (Eqs. 9-11), as follows:

$$\left(\frac{\dot{M}_{max}}{\dot{M}_{min}}\right)_{IJ} \approx \sqrt{1.85 + 0.85x^{-1}f_2^{-2}} \tag{6}$$

$$\left(\frac{\dot{M}_{max}}{\dot{M}_{min}}\right)_{II} \approx \sqrt{1.26 + 0.26x^{-1}f_2^{-2}} \tag{7}$$

$$\left(\frac{\dot{M}_{max}}{\dot{M}_{min}}\right)_{II} \approx \sqrt{1.13 + 0.13x^{-1}f_2^{-2}}$$
(8)

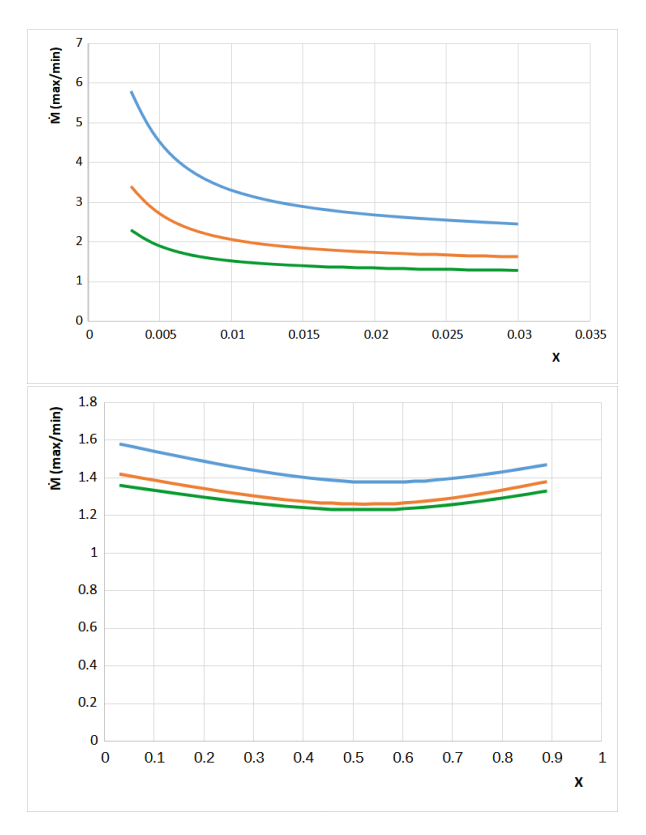


Fig. 3: Dimensionless distributions of the accretion rate deviations for the three observation nights. The distributions increase across the accretion disk, as presented: the UV-part (top panel) and the optical disk (bottom panel).

$$\left(\frac{\dot{M}_{max}}{\dot{M}_{min}}\right)_{B} \approx \sqrt{1.3 + 0.3x^{-1}f_{2}^{-2}}$$
 (9)

$$\left(\frac{\dot{M}_{max}}{\dot{M}_{min}}\right)_{B} \approx \sqrt{1.2 + 0.2x^{-1}f_{2}^{-2}}$$
 (10)

$$\left(\frac{\dot{M}_{max}}{\dot{M}_{min}}\right)_{B} \approx \sqrt{1.17 + 0.17x^{-1}f_{2}^{-2}}$$
 (11)

As we have explained earlier in this section, there are different types of activity in different parts of the disk. However, in the outer active zone, where advection suppresses the activity effects, a smooth decrease in the accretion rate variations is observed. After that, at x < 0.4, an increase in these distributions resumes (Fig.3, bottom panel). Fig.3 (top panel) shows that in all three runs in the UV-disk the values of the accretion rate fluctuations increase intensively towards the inner disk edge.

5 Discussion and Conclusions

In this paper, we have analyzed the short-time variability of the symbiotic star T CrB, and compared its behaviour in three nights of our observations.

From the results in Section 4 we can see that both in the outer contact zone and in the outer disk active zone, where the optical spectrum comes from, the increase of accretion rate deviations does not exceed 1.58 ± 0.02 (see Fig.3, bottom panel). This corresponds well to the average mass accretion from the observations. In contrast, in the inner active zone the deviations start to increase more intensively and in the inner UV disk, where the inner contact zone resides, it can reach 5.8 ± 0.2 (see Fig.3, top panel). These high values can be caused by the direct interaction of the inner disk regions with the accretor shell. It has been suggested (Yankova et al. 2025) that in this evolutionary stage the white dwarf has a well-formed shell. In general, the analysis of the results leads to the following conclusion: the observed flickering is directly related to the active zones in the disk and shows a typical behaviour in each of them.

Acknowledgments: The research infrastructure is supported by the Ministry of Education and Science of Bulgaria (Bulgarian National Roadmap for Research Infrastructure). The authors are grateful to the anonymous referee for the useful comments that helped us to improve our paper.

References

```
Allen, D.A., 1984, PASAu, 5, 369
Bailer-Jones, C.A.L., Rybizki, J., Fouesneau, M., Demleitner, M., Andrae, R., 2021, AJ, 161, 3, 147
Balbus S. A., Hawley J. F., 1998, Rev. Modern Phys., 70, 1
Belczynski, K., Mikolajewska, J. 1998, MNRAS, 296, 77
Boffin H.M.J., 2015, ASSL, 413, 153
Bruch A., 1992, A&A, 266, 237
Bruch A., Duschl W. J., 1993, A&A, 275, 219
Cassatella, A., Gilmozzi, R., Selvelli, P. L., 1985, ESA, SP, 236, 213
Dobrotka A., Hric L., Casares J., Shahbaz T., Martínez-Pais I. G., Muñoz Darias T., 2010, MNRAS, 402, 2567
Fekel, F. C., Joyce R. R., Hinkle K. H., Skrutskie M. F., 2000, AJ, 119, 1375
Frank, J., King, A., Raine, D. J., 2002, Accretion Power in Astrophysics:3rd Edition
```

```
Gromadzki, M., Mikolajewski M. Tomov T. Bellas-Velidis I. Dapergolas A. Galan C., 2006,
     Acta Astron., 56, 97
Henden, A., & Munari, U. 2006, A&A, 458, 339
Hric, L., Petrik, K., Urban, Z., Niarchos, P., and Anupama, G. C. 1998, A & A, 339, 449
Huggins, W., 1866, MNRAS, 26, pp. 275-7, 297
Iankova Kr.D., 2009, Publ. Astron. Soc. "Rudjer Bokovi", 9, 327-333 Kenyon, S. J., Garcia M. R., 1986, AJ, 91, 125
Kenyon S. J., 1990, ASPC, 9, 206
Lasota, J.P., 2001, NewAR, 45, 449
Leibowitz, E. M., Ofek E. O., Mattei J. A., 1997, MNRAS, 287, 634
Luna, G. J. M., Nelson, T., Mukai, K., Sokoloski, J. L., 2019, ApJ, 880, 94
Luna, G. J. M., Sokoloski, J. L., Mukai, K., and Kuin, N.P.M., 2020, ApJL, 902, L14
Miney, M., Petrov, N., & Semkov, E. 2024, Contributions of the Astronomical Observatory
     Skalnate Pleso, 54, 15
Munari U., 2019, Cambridge Astrophysical Series, 54, 77
Mürset, U. and Schmid, H. M., 1999, A & AS, 137, 473
Nikolov, Y. 2022, New Astronomy, 97, 101859
Payne-Gaposchkin, C., 1964, The Galactic Novae, Dover, New York
Rodrigo, C., & Solano, E. 2020, in XIV.0 Scientific Meeting (virtual) of the Spanish Astro-
     nomical Society, 182
Schaefer, B. E. 2022, MNRAS, 517, 6150
Schaefer, B., 2023, MNRAS, 524, 2, p.3146-3165
Selvelli, P. L., Cassatella, A., Gilmozzi, R. 1992, ApJ, 393, 289
Smak, J., 2000, NewAR, 44, 171
Stanishev, V., Zamanov, R., Tomov, N., Marziani, P. 2004, A&A, 415, 609
Straizys, V., 1992, Multicolor Stellar Photometry (Tucson: Pachart Pub House)
Sokoloski, J. L., Bildsten, L., and Ho, W. C. G., 2001, MNRAS, 326, 553
Tsvetkov, M.K., Georgiev, T.B., Bilkina, B.P., Tsvetkova, A.G., Semkov, E.H., 1987, Bol-
     garska Akademiia Nauk Doklady 40, 9
Warner B., Nather R. E., 1971, MNRAS, 152, 219
Warner, B., 2003, Cataclysmic variable stars, Vol. 28, Cambridge University Press
Webbink, R. F., Livio M., Truran J. W., Orio M., 1987, ApJ, 314, 653 Yankova, Kr., Filipov L., Boneva D., Gotchev D., 2014, BgAJ, 21, 74
Yankova, K., 2019, Proc. XIth SIMIA, p.60-64, https://ui.adsabs.harvard.edu/abs/2019simi.conf...60K/
Yankova, K., 2023, Publ. Astron. Soc. RudjerBokovi, No 25, p. 179-186
Yankova, K., 2025, Publ. Astron. Obs. Belgrade, No. 107, 139 - 144
Yankova, Kr., Boneva, D., Zamanov, R., 2025, Aerospace Research in Bulgaria, 37, p.30-39, DOI: https://doi.org/10.3897/arb.v37.e03
Zamanov R. K., Bruch A., 1998, A&A, 338, 988
Zamanov, R., Bode, M. F., Stanishev, V., and Martí, J. 2004, MNRAS, 350, 1477
Zamanov, R., Boeva, S., Latev, G., Semkov, E., Minev, M., Kostov, A., Bode, M. F., Marchev,
V., Marchev, D., 2023, A&A 680, L18
Zhekov S. A., Tomov T. V., 2019, MNRAS, 489, 2930
```